Two-dimensional viscous flow analysis in a micro flow-cell of an ultraviolet absorption detector for high-performance liquid chromatography

MASAO KAMAHORI*, YOSHIO WATANABE and HIROYUKI MIYAGI

Central Research Laboratory, Hitachi Ltd., 1-280 Higashikoigakubo, Kokubunji, Tokyo 185 (Japan)

and

HIROSHI OHKI and RYO MIYAKE

Mechanical Engineering Research Laboratory, Hitachi Ltd., 502 Kandatsu, Tsuchiura, Ibaraki 300 (Japan)

(First received July 5th, 1990; revised manuscript received October 30th, 1990)

ABSTRACT

Flow profiles in a Z-type 0.6-μl micro flow-cell of an ultraviolet absorption detector for high-performance liquid chromatography were evaluated. The flow profile and band broadening in the flow-cell were calculated by finite-element analysis using a supercomputer (HITAC S-810). The flow profile was Poiseuille flow following the Golay equation at flow-rates less than 0.2 ml/min. However, at flow-rates above 0.2 ml/min the flow had two types of band broadening, depending on the form of the flow-cell and the connection between the flow-cell and the connecting tubing. The first type was band broadening independent of flow velocity, including mixing broadening at flow-rates from 0.2 to 1.0 ml/min. The second was mixture-type band broadening between laminar flow broadening and mixing broadening depending on the flow velocity, which gave a Gaussian profile containing a tailing peak, at flow-rates over 1.0 ml/min. A comparison of these results and the experimental results showed good agreement.

INTRODUCTION

Extra-column contributions to band broadening are significant for overall system performance in high-performance liquid chromatography (HPLC). They become more and more critical when highly efficient fast and micro liquid chromatography using small particle packings or narrow-bore columns are employed [1]. They include volumetric broadening originating from the injector, detector flow-cell and connecting tubing and temporal broadening resulting from the response rate of the detector. In particular, the detector flow-cell is a significant source of band broadening in the chromatographic system.

Sternberg [2] reported that several sources of volumetric broadening were present in the flow-cell: the cell volume itself; laminar flow broadening; and mixing and diffusional broadening. Laminar flow broadening resulting from the laminar flow and an associated parabolic flow profile in the flow-cell has been described by Martin *et al.* [3]. It is generally recognized that when sharp diameter changes in fittings between

the flow-cell and the connecting tubing are present, in addition to abrupt bends in the flow-cell, band broadening may be caused. The band broadening is extremely difficult to describe from a purely theoretical basis, since it involves a poorly described area of hydrodynamics in the range of low Reynolds numbers, where laminar flow is normally expected. However, laminar flow broadening is usually an insignificant source of band broadening in the flow-cell because of its short length. Rather, the flow-cell often contributes to distortion or exponential tailing of a solute peak. One source may be the diffusional and mixing processes which occur within flow-cells containing a fitting and that also have abrupt bends. If the flow profile in the flow-cell is similar to that in open tubing, the flow profile in the Z-type flow-cell should be of the Poiseuille type in the main channel. This includes secondary flow or turbulence in the fitting. However, there is no theoretical explanation regarding band broadening in flow-cells that have the fitting and the abrupt bends, because the relevant Navier–Stokes differential equations for complex geometrical forms have not been solved. A careful design of the flow-cell in fast and micro HPLC requires detailed knowledge of the flow profiles and band broadening in the flow-cell.

Recently, Atwood and Golay [4,5] reported that the dispersion of a short tubing was mathematically simulated using a computer model combining a Poiseuille flow with diffusion. They studied the theory of dispersion in a sample in short, straight open tubings. However, they have not directly solved the relevant Navier–Stokes differential equations and the diffusion equation, but have used the model combining the Poiseulle flow with diffusion. It may be difficult to simulate dispersion of the Z-type flow-cell of an ultraviolet absorption detector because of its complex geometrical forms (*i.e.* an abrupt bend and a fitting with sharp changes in tubing diameter). Furthermore, it may not be possible to visualize the flow and concentration profiles in the flow-cell. In this paper, the simulation of flow profiles and band broadening in the Z-type flow cell with a direct solution of these equations by finite-element analysis using a supercomputer (HITAC S-810) is discussed.

EXPERIMENTAL

Practical measurements of band broadening in the flow cell

A Hitachi 655A-12 liquid chromatograph pump was used. The mobile phase was passed through a column (50 mm × 4 mm I.D.), packed with 2-μm glass beads, to the injector (Rheodyne 7520) by the pump. The injector was connected directly, without a separation column, to a modified Hitachi 655-51 UV monitor (with the reported 0.6-μl flow-cell [6]). The output signal from the UV detector was fed to an analyzing recorder (YEW Model 3655).

Methanol was used as the eluent, into which 0.5 μl of benzene (0.5%, v/v, dissolved in the eluent) was injected. Most of the measurements, because at very narrow band profiles, have to be carried out in less than 1 s, because practical measurements of band broadening were carried out without a separation column. We used a system that had an overall time constant of 10 ms for the detector electronics and a sampling rate of 1 ms with a 1-kHz low-pass filter for the recorder. The band broadening was defined by the standard deviation of a concentration profile, taking the width at 60.7% of the maximum height.

Two-dimensional viscous flow analysis in the flow-cell

To determine the real flow profiles in the flow-cell, it is necessary to solve a three-dimensional viscous flow analysis problem. However, it is not obvious that, to solve the relevant Navier–Stokes differential equations, a diffusion equation may be used to analyze the flow profiles in the flow-cell. Furthermore, three-dimensional viscous flow analysis is a complicated and time-consuming task. It was difficult to solve the flow analysis in this stage. In the first stage, two-dimensional viscous flow analysis, which is simpler than three-dimensional analysis but ignores the effect of flow and diffusion in the z direction (*i.e.* eddy diffusion), was applied directly to solve the flow profiles in the flow-cell. We have studied here the theory, in this case of two-dimensional flow analysis.

A computer program for two-dimensional viscous flow analysis using finite-element analysis has been developed by Ikegawa and co-workers [7–9]. A mathematical handling of the flow and concentration profiles is possible, but the chromatogram and variance (second moment) are not included in the program. We prepared a new program for calculation of the band broadening, that is the chromatogram and second moment, in the flow-cell. An outline of the calculation method is as follows.

Calculation of velocity vector

A simplified flow chart for the calculation of the velocity vector is shown in Fig. 1. The initial condition was a non-compressed viscous flow. First, potential flow in the flow-cell was calculated without the viscous effect. Secondly, the velocity vector was calculated using the results of the potential flow with the viscous effect. The flow profile was drawn using the calculated velocity vector.
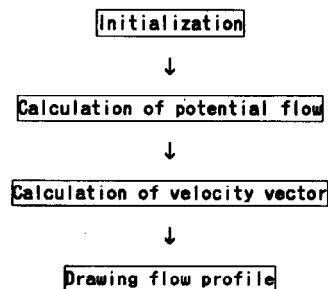

Fig. 1. Flow chart for calculation of flow profile.

Calculation of chromatogram and second moment

Fig. 2 shows a simplified flow chart for the calculation of the chromatogram and second moment. The initial condition was the input of the sample concentration profile. First, the diffusion equation was solved using the calculated velocity vector. Secondly, the chromatogram was drawn using the calculated concentration of each element in the flow-cell. Finally, the second moment was calculated.

Conditions for the calculation were as follows: number of elements, 3175; mobile phase, methanol; solute, benzene; diffusion coefficient, 0.001 mm^2/s; range of flow-rates, 0.2–2.0 ml/min.

Initialization

↓

Calculation of diffusion equation

↓

Calculation of concentration

↓

Calculation of chromatogram

↓

Drawing chromatogram

↓

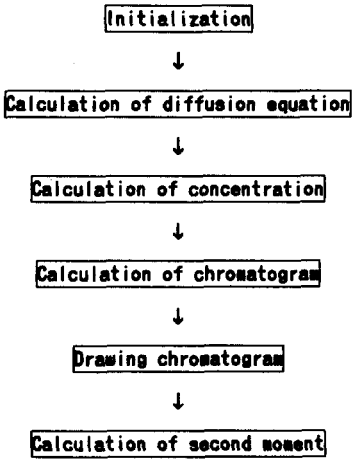| Calculation of second moment |
| :---: |

Fig. 2. Flow chart for calculation of chromatogram and second moment.

Fig. 3 shows the structure of the flow-cell for two-dimensional viscous flow analysis. Fig. 4 shows the mesh of the flow path in the flow-cell for the analysis corresponding to Fig. 3.
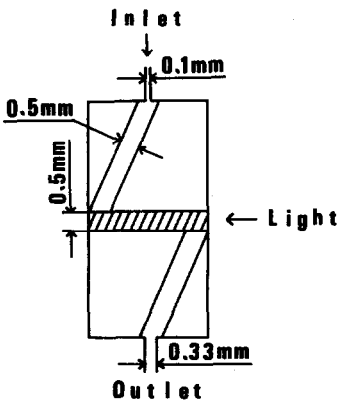

Fig. 3. Schematic diagram of flow-cell. Oblique lines indicate optical path.
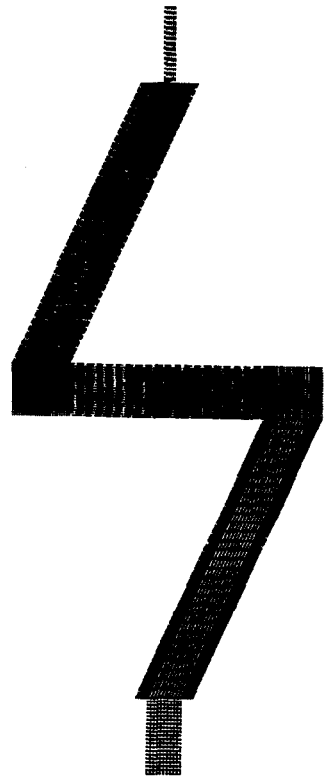
Fig. 4. Mesh of flow-cell for finite-element analysis.

TABLE I

TYPES OF BAND BROADENING IN CHROMATOGRAPHIC SYSTEM

Symbols: r = cell radius; L = cell length; F = solvent flow-rate; D_m = solvent diffusion coefficient; V = cell volume.

Type of band broadening	Response function	Second moment (σ^2)
Laminar flow broadening		$\pi\, r^4\, LF/24 D_m$
Diffusional broadening		$L^4 F^2/4 D_m{}^2$
Mixing broadening		V^2

RESULTS AND DISCUSSION

Basic theory

The detector flow-cell is a significant source of band broadening within the chromatographic system. Sternberg [2] suggested that the flow-cell has several sources of volumetric broadening: the cell volume itself; laminar flow broadening; and mixing and diffusional broadening. The different types of volumetric broadening, the corresponding response functions and their second moments expressed as the volume-based variance are summarized in Table I. The listed data show that laminar flow broadening is Gaussian, and diffusional and mixing broadening are exponential.

Band broadening

Fig. 5 shows a plot of actual variance (closed circles) *versus* flow-rate for the flow-cell. Four types of band broadening phenomena exist according to the flow-rate (F): (1) $F \leqslant 0.25$ ml/min: the variance increased with increasing flow-rate; (2) 0.25 ml/min $\leqslant F \leqslant 0.4$ ml/min: the variance decreased slightly with increasing flow-rate; (3) 0.4 ml/min $\leqslant F \leqslant 1.0$ ml/min: the variance was constant, independent of the

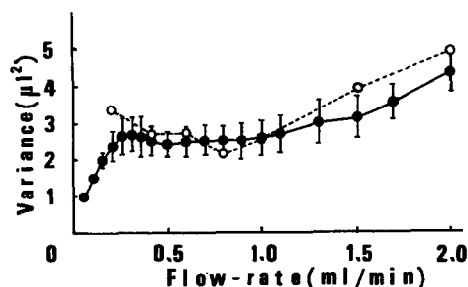

Fig. 5. Effect of flow-rate on variance. Symbols: ● = actual variance; | = standard deviation; ○ = calculated variance.

flow-rate; (4) 1.0 ml/min $\leqslant$ *F*: the variance increased with increasing flow-rate, but the slope of the line was different from that at flow-rates less than 0.25 ml/min.

In a previous paper [6], we reported on the flow dependency in the micro flow-cell. The flow dependency found in the two studies differed. The difference may result from the injector and the connecting tubing, because the Rheodyne injector had much smaller broadening than the former one used (Tokyorika 5001). The connecting tubing in this study was 20 mm × 0.1 mm I.D. and smaller than the 20 mm × 0.25 mm I.D. tubing used in the previous study. So the flow dependency seen in the present case should be very close to the actual contribution of band broadening in the flowcell.

Fig. 5, as mentioned before, shows a plot of the calculated variance (open circles) *versus* flow-rate for the flow cell. We have studied fast HPLC, and made a computer program for it. Therefore, there are no data for the calculated variance at flow-rates less than 0.2 ml/min in this study, because the computer program for flow analysis needs another key to solve variance for low flow-rates. Three types of band broadening phenomena were apparent: (1) 0.2 ml/min $\leqslant$ *F* $\leqslant$ 0.4 ml/min: the variance decreased slightly with increasing flow-rate; (2) 0.4 ml/min $\leqslant$ *F* $\leqslant$ 1.0 ml/min: the variance was constant, independent of the flow-rate; (3) 1.0 ml/min $\leqslant$ *F*: the variance increased with increasing flow-rate.

The actual measurements and calculation of band broadening are summarized in Table II. A comparison of the experimental and calculated results showed good agreement.

TABLE II

DEPENDENCE OF BAND BROADENING ON FLOW-RATE

Flow-rate (ml/min)	Band broadening	
	Experiment	Calculation
< 0.2	Increase	–
0.2–0.4	Slightly decrease	Slightly decrease
0.4–1.0	Constant	Constant
> 1.0	Increase	Increase

Simulated flow profiles and chromatogram

Fig. 6a, b and c show the flow profile in the flow-cell at flow-rates of 0.2, 0.6 and 2.0 ml/min, respectively. Atwood and Golay [5] reported that the peak eluted from a small injection becomes markedly non-Gaussian in a short straight tubing because of insufficient velocity averaging. At the flow-rate of 0.2 ml/min, however, the flow profile was Poiseuille flow following the Golay equation [10], as shown in Fig. 6a. The band broadening was the laminar flow type. The velocity averaging (*i.e.* sample molecular averaging) requires long tubing or a high flow-rate if the tubing used is straight and round. The result of this study may indicate that the velocity averaging occured in the fitting with sharp changes in tubing diameter in spite of having short tubing with low plate numbers. In fact, the calculated chromatogram was nearly
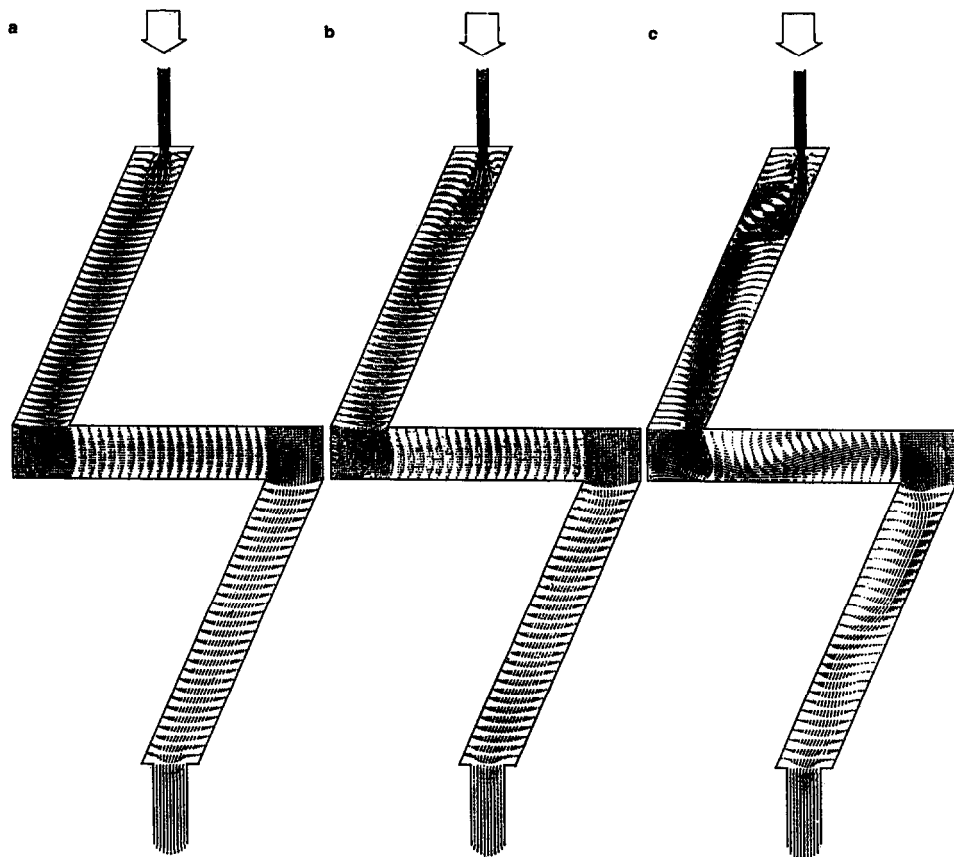
Fig. 6. Calculated flow profile in flow-cell. Flow-rates: (a) 0.2 ml/min, (b) 0.6 ml/min, (c) 2.0 ml/min.

Gaussian at the flow-rate of 0.2 ml/min (data shown later). At flow-rates from 0.2 to 1.0 ml/min, the flow had a parabolic profile in the main channel, which included an eddy current in the fitting between the flow-cell and the connecting tubing. Additionally, stagnation occurred in the bend of the flow-cell, as shown in Fig. 6b. The eddy current in the fitting expanded with increasing flow-rate, including mixing broadening. The total band broadening in the flow-cell acted not as laminar flow broadening, but as mixing broadening owing to the eddy current in the fitting and to the stagnation in the bend due to the lower flow-rate. The second moment was constant, independent of the flow-rate. At flow-rates over 1.0 ml/min, the calculated second moment increased with increasing flow-rate. It was expected that laminar flow broadening, resulting from the laminar flow, and the associated parabolic flow profile in the flow-cell may exist. However, the parabolic flow profile in the main channel was transformed, and the eddy current in the fitting and the bend were as shown in Fig. 6c. Fig. 7 shows time courses of the concentration profiles in the flow-cell at a flow-rate of 1.0 ml/min. From the concentration profiles, the concentration distribution
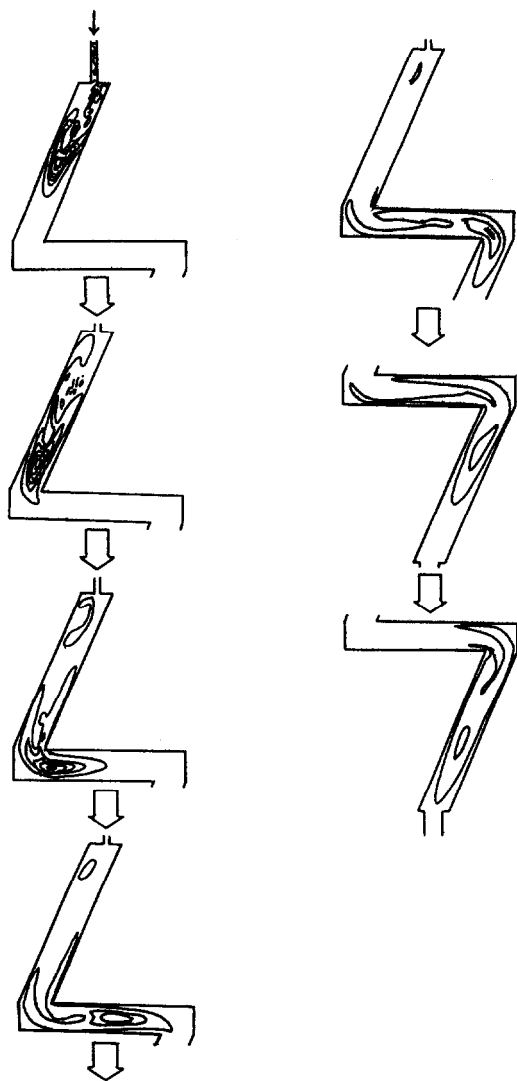
Fig. 7. Time courses of calculated concentration profiles in flow-cell.

was seen as separated, which led to a tailing peak. This case should be treated in terms of the Gaussian distribution, combined with essentially the Gaussian-broadened exponential distribution. The band broadening in such a peak would be approximated by a combination of laminar flow broadening and exponential broadening.

Fig. 8a–g shows a simulated chromatogram by finite-element analysis at flow-rate of 0.2, 0.4, 0.6, 0.8, 1.0, 1.5 and 2.0 ml/min, respectively. The calculated chromatogram at the flow-rate of 0.2 ml/min was nearly Gaussian, as shown in Fig. 8a. An increasing flow-rate led to formation of the tailing peak, which indicated enlargement
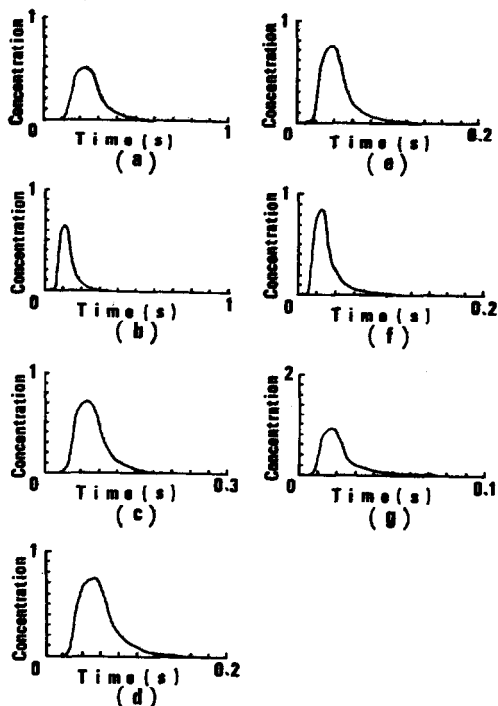
Fig. 8. Calculated chromatogram by finite-element analysis. Flow-rates: (a) 0.2 ml/min; (b) 0.4 ml/min; (c) 0.6 ml/min; (d) 0.8 ml/min; (e) 1.0 ml/min; (f) 1.5 ml/min; (g) 2.0 ml/min.

of the effect on mixing broadening caused by the eddy current and the stagnation. In particular, the calculated chromatogram at the flow-rate of 2.0 ml/min produced an exponential peak more than half that shown in Fig. 8g. In the case of the actual chromatogram, the profile generally showed an extended tailing peak with increasing flow-rate. A comparison of both results showed good agreement.

A plot of the eluted volume of the mobile phase *versus* flow-rate for the flow-cell is shown in Fig. 9. At flow-rates from 0.2 to 0.8 ml/min, the eluted volume was nearly
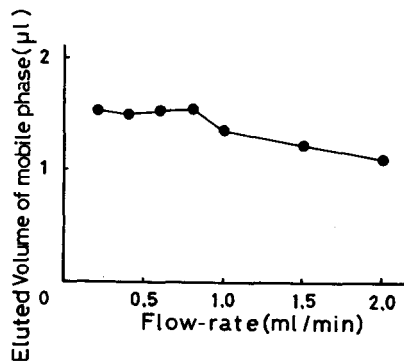

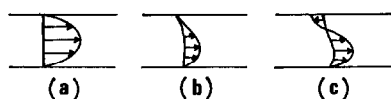Fig. 9. Effect of flow-rate on eluted volume of mobile phase.

Fig. 10. Types of band broadening in flow-cell. (a) Laminar flow broadening; flow-rates less than 0.2 ml/min; (b) intermediate state; flow-rates from 0.2 to 1.0 ml/min; (c) laminar flow broadening + mixing broadening; flow-rates greater than 1.0 ml/min.

constant, independent of the flow-rate. At flow-rates greater than 1.0 ml/min, the eluted volume decreased with increasing flow-rate. An ideal laminar flow would have a Gaussian profile whose variance would decrease with increasing flow-rate. The results also indicated that the eddy current resulted in the constant variance at flow-rates from 0.2 to 1.0 ml/min, and the laminar flow controlled the variance at flow-rates greater than 1.0 ml/min.

Type of band broadening

The above-mentioned results may indicate that three types of band broadening existed in the Z-type micro flow-cell. Fig. 10a, b and c shows three types of band broadening at flow-rates less than 0.2, from 0.2 to 1.0, and greater than 1.0 ml/min. The first, Fig. 10a, was laminar flow broadening following laminar flow at flow-rates less than 0.2 ml/min. The second, Fig. 10c, was a mixture between laminar flow broadening and mixing broadening at flow-rates greater than 1.0 ml/min. The third, Fig. 10b, was an intermediate state between the first and second types at flow-rates from 0.2 to 1.0 ml/min. The intermediate state is affected by the form of the flow-cell, particularly the fitting between the flow-cell and the connecting tubing, and the bend in the flow-cell. Thus, the flow dependency in this study was suggested to be different from that in the previous study [6].

The flow-cell has more or less an exponential tail owing to the presence of tail-producing sites which lead to skewed peaks. The major source in this case was suggested to be the mixing process which occurred in the flow-cell containing the fitting and the bend. The two-dimensional viscous flow analysis can take into account band broadening in the flow-cell or even the fitting with sharp changes in tubing diameter, as well as the bend in the flow-cell.

The present numerical technique for two-dimensional viscous flow analysis by supercomputer is seen as a powerful tool for the design of various kinds of manufactured products, especially instruments in fast HPLC, which are related in design to fluid flow problems.

REFERENCES

 1 M. Verzele and C. Dewaele, in F. Bruner (Editor), *The Science of Chromatography*, Elsevier, Amsterdam, 1983, pp. 435–447.
 2 J. C. Sternberg, *Adv. Chromatogr.*, 2 (1966) 205–270.
 3 M. Martin, C. Eon and G. Guiochon, *J. Chromatogr.*, 108 (1975) 229–241.
 4 M. J. E. Golay and J. G. Atwood, *J. Chromatogr.*, 186 (1979) 353–370.
 5 J. G. Atwood and M. J. E. Golay, *J. Chromatogr.*, 218 (1981) 97–122.
 6 M. Kamahori, Y. Watanabe, J.Miura, M. Taki and H. Miyagi, *J. Chromatogr.*, 465 (1989) 227–232.
 7 M. Ikegawa and N. Sato, *Proceedings of the 7th Symposium on Numerical Analysis in Fluid Mechanics, Tokyo, Aug. 1986*, Union of Japanese Scientists and Engineers, Tokyo, 1986, , pp. 205–212.
 8 C. Kato and M. Ikegawa, *Proceedings of the 7th Symposium on Numerical Analysis in Fluid Mechanics, Tokyo, Aug. 1986*, Union of Japanese Scientists and Engineers, Tokyo, 1986, pp. 125–132.
 9 C. Kato and M. Ikegawa, *Proceedings of the 1st Symposium on Computational Mechanics, Tokyo, Aug. 1987*, Union of Japanese Scientists and Engineers, Tokyo, 1987, pp. 111–118.
10 M. J. E. Golay, in D. H. Desty (Editor), *Gas Chromatography 1958*, Academic Press, New York, 1958, 36–53.